Advances in Science and Technology Research Journal

Advances in Science and Technology Research Journal, 2026, 20(4), 317–327
https://doi.org/10.12913/22998624/215203
ISSN 2299-8624, License CC-BY 4.0

Received: 2025.11.21
Accepted: 2026.01.05
Published: 2026.03.01

Heuristic and machine learning methods for optimizing magnetorheological brake performance

Areg Grigoryan[1], Armine Avetisyan[1*], Tatevik Melkonyan[1], Mariam Gulinyan[1]

[1] Automation and Electromagnetic Systems Research Laboratory, National Polytechnic University of Armenia, Armenia
* Corresponding author's e-mail: e-mail: arm.avetisyan@seua.am

ABSTRACT

This study presents optimization techniques aimed at improving the performance of magnetorheological (MR) brakes through the application of heuristic algorithms and machine learning methods. MR fluids, characterized by their rapid and reversible transition between fluid and semi-solid states under the influence of a magnetic field, are widely used in automotive systems, robotics, and vibration control applications. The research focuses on optimizing key performance metrics – namely, the electromagnetic force acting on the front of the MR fluid magnetic particle bridge and the velocity of the bridge front – using both single- and multi-objective optimization approaches. Two distinct methodologies were employed: (i) heuristic methods using an automated system based on the mathematical model of the electromagnetic system, and (ii) hybrid methods combining machine learning models with heuristic algorithms. The results demonstrate that machine learning-assisted optimization substantially reduces computational time while maintaining high predictive accuracy. Furthermore, multi-objective optimization identified optimal structural dimensions and voltage levels that achieve balanced performance across the selected criteria. These findings highlight the potential of hybrid optimization strategies for the efficient design of MR brake systems, supporting their broader integration into advanced engineering applications.

Keywords: magnetorheological fluid, electromagnetic brake, hybrid optimization, heuristic algorithms, machine learning.

INTRODUCTION

Magnetorheological (MR) fluids are smart materials capable of undergoing rapid and reversible transitions from a liquid to a semi-solid state in the presence of a magnetic field. This unique property has led to the development of various MR fluid-based devices for applications ranging from automotive and aerospace engineering to civil infrastructure and medical systems. The growing interest in MR-based systems has especially centered on enhancing their controllability, performance, and efficiency through optimal structural design and control strategies. This section reviews recent advancements in MR fluid-based systems and emphasizes the optimization approaches applied across a wide array of devices, grouped thematically as follows.

MR dampers are among the most widely studied MR devices, used in vibration suppression, vehicle suspension, seismic mitigation, and energy absorption systems. Researchers have developed diverse structural configurations such as bypass dampers [1], valve-mode dampers with annular and radial gaps [2], double-ended [3] and hybrid designs [4], and systems with elastomer or smart sealing elements [5–7]. These studies aim to improve damping force, dynamic range, and responsiveness while minimizing energy consumption and structural volume. Advanced structural modeling and experimental validation have enabled significant improvements in damper performance, as demonstrated in studies focusing on low-velocity sensitivity [1], flow path expansion [8], temperature dependence [9], and topology optimization of elastomer cores [10]. Additionally, multi-physics

simulation frameworks and surrogate modeling techniques have provided accurate prediction capabilities and reduced computational costs in optimization [11-12].

MR brakes offer controllable and compact alternatives to traditional mechanical braking systems, especially in automotive, aerospace, and robotic applications. Several novel MR brake configurations have been proposed, including cylindrical brakes with dual fluid channels [13], rotor-integrated electromagnets [14], multi-disc and drum structures [15] comb-type disc configurations [16], squeeze-shear mode designs [17], and axial flux machine integrations [18, 19]. Performance optimization efforts have focused on enhancing torque output, minimizing brake mass, and improving response time and thermal characteristics [20-21]. Multi-objective genetic algorithms (GA, NSGA-II), particle swarm optimization (PSO), and approximate modeling techniques are widely used for dimensional and material parameter optimization of MR brakes [21].

MR valves control the flow of MR fluid within systems and are essential for adjustable damping in actuators and mounts. Studies have examined radial MR valves with annular and radial flow paths [22], geometrically optimized configurations using feedforward neural networks [23] and Taguchi-RSM models [24]. These works have enabled improvements in pressure drop, magnetic flux density, and dynamic response. MR mounts, especially those with multi-channel designs, are gaining traction in applications involving vibration isolation, such as engine mounting and medical equipment. A novel multi-channel MR mount structure was introduced with advanced controllability across a wide frequency range [25], while compact MR mounts with high force-to-volume ratios have been designed for use in automotive applications [26].

In the field of actuators, spherical MR actuators have been proposed for haptic applications [27], and torsional vibration absorbers with different coil configurations have been optimized for automotive engines [28]. MR mounts and dampers have also been applied in aircraft landing gear systems and washing machines [29, 30].

In addition to structural and application-specific developments, recent research has increasingly emphasized accurate magnetic characterization of MR fluids, high-fidelity field modeling, and data-driven parameter prediction as prerequisites for effective optimization. A compact neural-network-based model has been developed to reproduce the nonlinear dependence of relative magnetic permeability on magnetic flux density with an error of approximately 8%, demonstrating the suitability of radial basis function (RBF) neural network architectures for representing complex MR behavior [31, 32]. An automated permeability-measurement platform has also been introduced, combining microcontroller-based acquisition, synchronized dual-oscilloscope sampling, and frequency-swept excitation, thereby revealing the sensitivity of MR fluid magnetization to operating frequency and highlighting the need for high-resolution experimental datasets for predictive model development [33]. The importance of accurate modeling in transmittable -torque systems has further been demonstrated through the experimental characterization of a multidisc MR clutch, where Finite Element Method (FEM)-assisted analytical torque models follow laboratory measurements with an average deviation of approximately 7%, validating FEM--based methodologies for control and optimization [34]. More recently, MR fluids have been integrated into energy-harvesting magnetic-spring systems, where their high permeability and controllable rheology enhance magnetic flux density, displacement response, and harvested power, particularly in the low-frequency range relevant to ambient vibrations [35]. Collectively, these studies demonstrate that precise MR fluid characterization, supported by data-driven modeling and rigorous experimental validation, forms a critical foundation for the next generation of optimized MR devices across damping, braking, actuation, and energy-conversion applications.

The enhancement of MR devices heavily relies on advanced optimization strategies. Multi-objective evolutionary algorithms such as NSGA-II [5, 23, 36, 37], differential evolution (DE) [11], Grey Wolf pptimization (GWO) [10], JAYA [3, 38], and the iteration dependent optimizer (IDO) [39] have been applied for structural and control parameter optimization. In [5], NSGA-II was used to refine the structural characteristics of an MR fluid–elastomer damper, producing a well-distributed Pareto set that balanced damping force, dynamic range, and power consumption under multi-physics constraints. In [23], a feedforward neural network trained on finite-element magnetostatic data was incorporated into a hybrid optimization scheme combining genetic algorithms with sequential quadratic programming, significantly reducing computational cost

while enabling accurate geometric optimization of MR valves. System-level improvements were demonstrated in [36], where NSGA-II and MOST algorithms were used to optimize a tapered-flow-mode MR damper for vehicle suspensions, achieving notable reductions in vehicle roll and improved handling stability. A related study [37] applied NSGA-II to maximize dynamic range while minimizing coil turns, with final parameter selection guided by minimum-mass criteria; magnetic simulations and experiments confirmed the efficiency of the optimized design. In applications subject to strict geometric constraints, [11] proposed a multi-objective structural optimization method for a hybrid fluid-flow MR damper, leading to measurable gains in damping force and adjustable range alongside reduced energy consumption. Several modern metaheuristics were compared in [3], where JAYA and GWO outperformed GA in maximizing damping force based on CFD-supported statistical modeling and ANOVA-driven variable selection. Optimization of magnetostatic behavior was further explored in [38], where JAYA, GWO, and gradient-based methods were applied to a multi-coil MR valve; sensitivity analyses revealed that coil arrangement and non-magnetic spacers significantly affect magnetic flux density. Finally, [39] introduced the Iteration Dependent Optimizer, a nonlinear swarm-intelligence algorithm whose performance on benchmark problems was validated through its successful application to parameter identification of large-scale MR dampers used in structural control. Collectively, these studies demonstrate that advanced evolutionary algorithms, hybrid optimization frameworks, and surrogate modeling techniques play a critical role in improving the functional performance, efficiency, and controllability of MR-based devices.

Hybrid approaches also combine global and local search mechanisms to further enhance optimization efficiency – for example, genetic algorithms coupled with sequential quadratic programming (SQP) [21, 23] or hybrid Taguchi-based models [24, 40]. In addition, control-oriented optimization has advanced significantly through strategies such as PID tuning via GA, enhanced grey wolf optimization algorithms (EGWOA) [41], and neural network-based adaptive controllers [20, 42], all of which improve the responsiveness and stability of MR systems under dynamic operating conditions.

The collective efforts of researchers across the globe highlight a clear trend: the performance of MR fluid-based systems can be significantly enhanced through optimized design, advanced modeling, and intelligent control. These approaches address the challenges of power efficiency, response time, controllability, and miniaturization across a broad spectrum of MR devices. As optimization algorithms become more sophisticated and computational modeling more accessible, MR technology is poised for broader application and deeper integration into smart engineering systems. Building upon this foundation, the present article focuses on optimizing the performance of MR brakes through the application of heuristic algorithms and machine learning techniques, forming a hybrid optimization strategy.

MATERIALS AND METHODS

In the studied MR brake (Figure 1), the gap between the stationary stator and the rotating rotor is filled with MR fluid. When there is no magnetic field (i.e., no current flows through the control coil), the magnetic particles in the fluid are randomly distributed, and the fluid does not resist the rotor's rotation. However, when the control coil is connected to a power supply with voltage U, a magnetic field is generated by the electric current, and under the influence of the resulting electromagnetic force, the magnetic particles form chains that aggregate into a bridge structure [43, 44]. This bridge can be visualized as elongating under the influence of the magnetic field, with its front shifting from the rotor surface toward the stator surface [43]. As a result, the bridge connects the rotor to the stator and enables the transmission of braking torque.

Figure 2 illustrates the characteristic regions of the magnetic circuit [43]. The mean magnetic flux path generated by the magnetomotive force of the control coil can be divided into four characteristic regions (Figure 2): the rotor (regions 1 and 2), the MR-fluid gap (region 3), and the ferromagnetic stator (region 4). It is assumed that, at the current moment, the bridge has not yet reached the stator surface – that is, the front of the particle bridge has not fully developed across the gap. Consequently, Region 3 is subdivided into two zones: one occupied by the particle bridge and the other by the fluid.

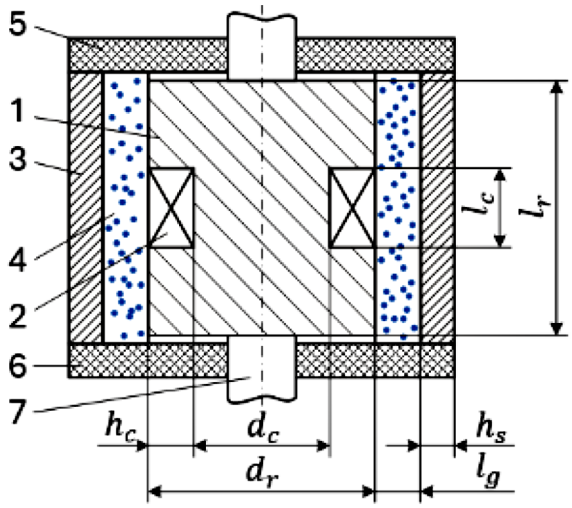

Figure 1. Schematic of the MR brake:
1 – ferromagnetic rotor, 2 – control coil,
3 – ferromagnetic stator,
4 – MR fluid with magnetic particles,
5,6 – non-magnetic cover, 7 – shaft

Based on the magnetic flux distribution, a magnetic equivalent circuit (MEC) of the brake was formed in [43], providing the foundation for deriving the mathematical model. The model assumes that a portion of the magnetic particles in the MR fluid are cubic, while the rest are spherical in shape. The resulting system of equations includes both linear and nonlinear components. This model allows for solving both the direct and inverse problems of the magnetic circuit. Specifically, if the magnetic flux Φ of the magnetic circuit is known, the magnetomotive force F in the control coil can be determined (direct problem), and vice versa, if F is given, Φ can be calculated (inverse problem) [43]. In the process of solving these problems, additional parameters of the brake and the magnetic circuit are determined. For instance, solving the inverse problem enables the calculation of the electromagnetic force P_E acting on the front of the particle bridge, which is responsible for elongating the bridge, as well as the velocity v of the bridge front moving toward the stator surface [43, 44]. In [43], a parametric analysis of the mathematical model demonstrated its adequacy and validated its consistency with the physical phenomena observed in the electromagnetic system of the brake.

In [44] two single-objective optimization problems are formulated under the condition F=*const*, where key performance indicators P_E and v are selected as the objective functions. These quantities are of particular importance, as they directly influence the response speed of the brake system:

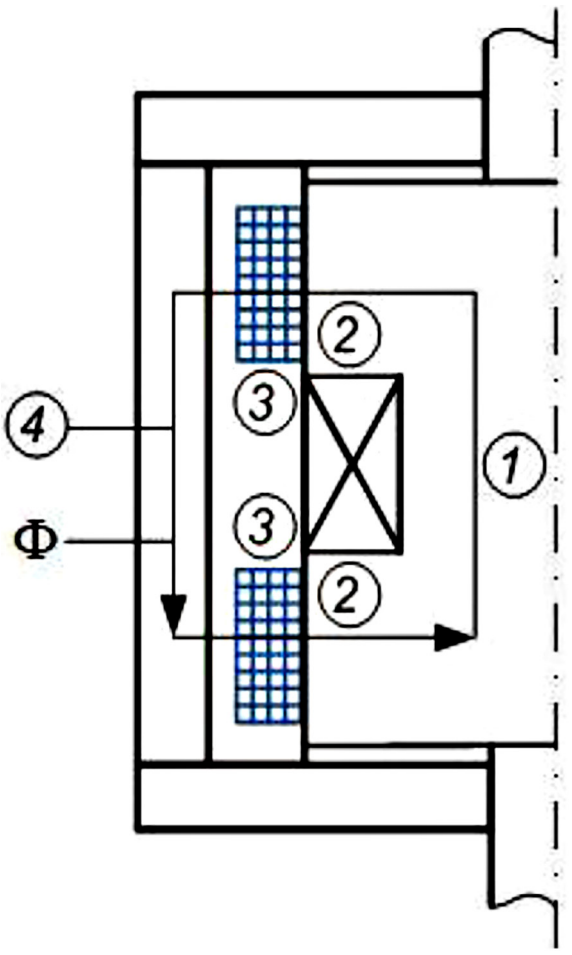

Figure 2. Characteristic regions of the magnetic flux path

$$P_E(d_r, h_s, h_c, l_r, l_c, U) \rightarrow max \quad (1)$$

$$v(d_r, h_s, h_c, l_r, l_c, U) \rightarrow max. \quad (2)$$

The optimization problems are subject to the following constraints for structural parameters d_r, h_s, h_c, l_r, l_c (Figure 1) and voltage U:

$$\begin{cases} 0.034 \le d_r \le 0.042, \\ 0.0031 \le h_s \le 0.0039, \\ 0.007 \le h_c \le 0.0085, \\ 0.028 \le l_r \le 0.034, \\ 0.01 \le l_c \le 0.012, \\ U = [12, 24, 48\,]. \end{cases} \quad (3)$$

Along with solving the optimization problems, the heating temperature of the control coil was also determined. This temperature was constrained by the maximum allowable heating temperature of the coil, which was set to 180 °C based on calculations performed for an AWG wire.

The described optimization tasks were formulated as nonlinear discrete programming

problems, since the voltage U can take on three discrete values, and both P_E and v are obtained through the solution of nonlinear models. The authors previously solved these optimization tasks using a genetic algorithm, as described in [44], where the objective function values were predicted using machine learning models trained on a dataset of approximately 650,000 brake design variants. The genetic optimization and machine learning algorithms were also applied by the authors to the optimal design of an electromagnet with a straight armature [45].

Given the complexity of the objective functions and the absence of gradient information, heuristic search-based, derivative-free optimization algorithms were employed in this study. Specifically, the coordinate descent and hyperspherical random search methods were used due to their suitability for high-dimensional and nonlinear optimization landscapes, such as those encountered in the design of MR brakes. These methods enabled efficient exploration of the design space, balancing local refinement with global search, and thereby supporting the identification of optimal geometrical and electrical parameters for the brake system.

OPTIMIZATION STRATEGY AND RESULTS

In the present study, two distinct approaches were employed to solve the single-objective optimization problems associated with the MR brake. In the first approach, the objective function values were computed using an automated simulation system [46], which integrated both the direct and inverse models of the electromagnetic circuit. In the second approach, the objective function values were predicted using a pre-trained machine learning model developed from a previously constructed dataset [44]. The following sections present the optimization results obtained from both approaches for the two objective functions defined in problems (1) and (2).

Optimization results using the automated system

Optimization problems (1) and (2) were solved using two heuristic algorithms: coordinate descent (CD) and hyperspherical search (HS). Multiple trials were conducted, and representative results for problem (1) are presented in Table 1. The table summarizes the optimal value of the objective function (P_E*), the corresponding optimal structural parameters (d_r*, h_s*, h_c*, l_r*, l_c*), the optimal applied voltage (U*), the number of iterations (Iter.), and the computational time (Time). All optimization tasks were executed on a system equipped with an Intel(R) Core™ i9-14900K processor and NVIDIA GeForce RTX 4070 graphics card. The evolution of the objective function values over the course of iterations for the second trial in Table 1 is illustrated in Figure 3.

Results for problem (2) are summarized in Table 2, which presents the optimal value of the objective function (v*), the corresponding optimal structural parameters and voltage, as well as the number of iterations and the total computational time. Figure 4 illustrates the evolution of the objective function values across iterations for the first trial listed in Table 2.

Table 1. Optimization results for problem (1)

N	Method	Optimal solution			Time, s	Iter.
		P_E*, N	(dr*, hs*, hc*, lr*, lc*), m	U*, V		
1	CD	43.2525	(0.04199994, 0.0039, 0.007, 0.034, 0.010003)	48	18.71	58
	HS	42.0106	(0.0406627, 0.00389995, 0.00700483, 0.03399979, 0.01000013)	12	154.74	109
2	CD	43.2525	(0.04199994, 0.0039, 0.007, 0.034, 0.010003)	24	18.92	58
	HS	43.2457	(0.04199542, 0.00389870, 0.00700109, 0.03399995, 0.01000002)	12	115.39	74
3	CD	43.2525	(0.04199994, 0.0039, 0.007, 0.034, 0.010003)	24	20.58	60
	HS	42.2162	(0.04197885, 0.00372557, 0.00703627, 0.03334219, 0.01011817)	12	108.41	64

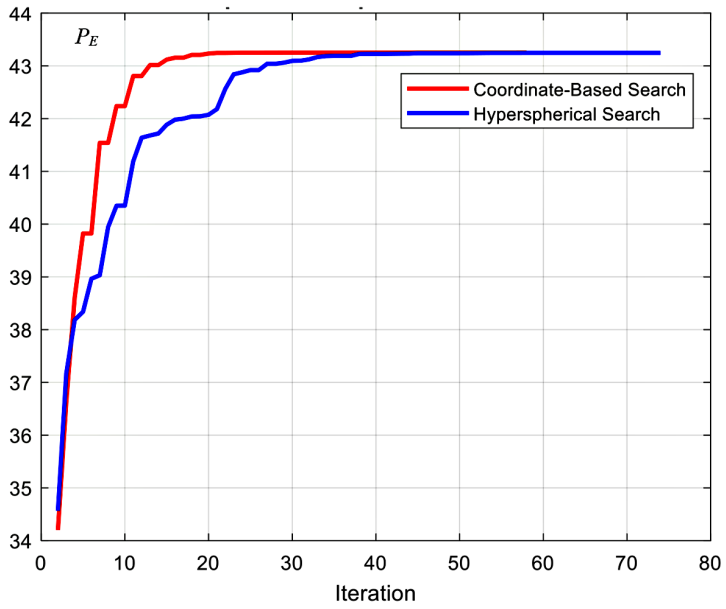

Figure 3. Evolution of the objective function P_E

Table 2. Optimization results for problem (2)

N	Method	Optimal solution			Time, s	Iter.
		v*, m/v	(dr*, hs*, hc*, lr*, lc*), m	U*, V		
1	CD	82.3225	(0.03901953, 0.0039, 0.007, 0.02800003, 0.012)	24	24.05	64
	HS	82.3004	(0.03954004, 0.00381954, 0.00700096, 0.02800173, 0.01199827)	12	153.04	87
2	CD	82.3225	(0.03901953, 0.0039, 0.007,0.02800003, 0.012)	48	24.31	64
	HS	82.3099	(0.03824126, 0.00381597, 0.00700076, 0.02800163, 0.01199152)	12	102.27	55
3	CD	82.3225	(0.03901953, 0.0039, 0.007, 0.02800003, 0.012)	24	24.33	64
	HS	82.3197	(0.03804656, 0.00389656, 0.00700073, 0.02800004, 0.01198507)	12	116.41	60

Optimization results using machine learning

The optimization results for problems (1) and (2) were also obtained using machine learning-assisted methods, in which the objective function values were predicted by trained models. According to the authors' prior work [44], the highest prediction accuracy for the objective function P_E was achieved using a tri-layered neural network (TNN) with three hidden layers of size (10, 10, 10)-constructed and validated in MATLAB's machine learning and deep learning apps (regression learner). This model produced an R-squared value of 0.998891329. Consequently, the TNN model was adopted to predicting P_E values during the optimization process. For predicting the v objective function, the best performance was obtained using the Fine Tree method – also generated using MATLAB's Regression Learner, which achieved an R-squared value of 0.991182994. Given its high predictive accuracy, this model was selected for the optimization task associated with the bridge-front velocity. Table 3 presents the representative results for problem (1), including the optimal value of P_E, the associated optimal structural parameters and voltage, as well as the number of iterations and computational time required for convergence.

The optimization results for problem (2) are summarized in Table 4, which presents the optimal value v^*, the corresponding optimal parameters, and the relevant performance metrics.

Multi-objective optimization results

In engineering design problems, it is often necessary to optimize multiple criteria simultaneously rather than treating them separately. To maximize overall performance, a generalized objective

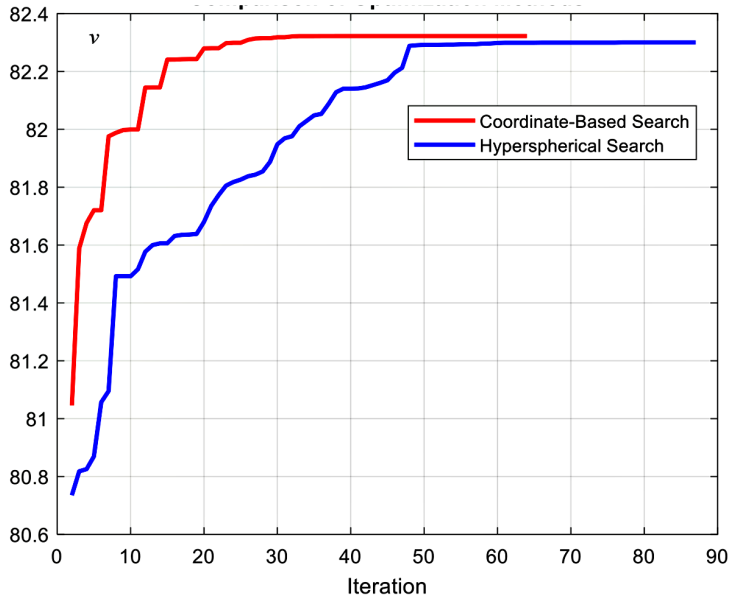

Figure 4. Evolution of the objective function v

Table 3. Optimization results for problem (1)

N	Method	Optimal solution			Time, s	Iter.
		P_E*, N	(dr*, hs*, hc*, lr*, lc*), m	U*, V		
1	CD	42.8728	(0.042, 0.0039, 0.007, 0.034, 0.01)	48	0.61	55
	HS	42.8724	(0.042, 0.0039, 0.00700042, 0.034, 0.01)	12	6.73	164
2	CD	42.8728	(0.042, 0.0039, 0.007, 0.034, 0.01)	24	0.55	55
	HS	42.8728	(0.042, 0.0039, 0.007, 0.034, 0.01)	12	7.32	182
3	CD	42.8728	(0.042, 0.0039, 0.007, 0.034, 0.01)	12	0.69	66
	HS	42.8284	(0.042, 0.0039, 0.00705399, 0.034, 0.01)	12	5.79	151

function was constructed by integrating the previously defined optimization problems (1) and (2):

$$\sigma = \left(\frac{P_E - P_E^*}{P_E^*}\right)^2 + \left(\frac{v - v^*}{v^*}\right)^2 \rightarrow \min \qquad (4)$$

where: P_E*=43.2525N *and* v*=82.3225 *m/v.*

This multi-objective optimization problem was solved using machine learning-assisted optimization. Applying the coordinate descent method, the optimal structural parameters of the MR brake were determined as $(d_r^*, h_s^*, h_c^*, l_r^*, l_c^*)$ = (0.042, 0.0039, 0.007, 0.034, 0.010125) with an applied voltage of U=12V. The corresponding performance metrics were P_E=42.6750N and v=80.5224 m/s. These results were validated using the hyperspherical method, which produced identical outcomes. The value of the generalized objective function (4) at this optimum was found to be 0.0004. Figure 5 illustrates the convergence of the generalized objective function values across iterations.

Analyses of optimization strategies and results

The results indicate that both traditional optimization techniques and machine learning-assisted approaches offer unique advantages, depending on the specific requirements of the problem, such as computational efficiency, accuracy, and scalability.

The heuristic methods demonstrated robustness in identifying optimal structural parameters and voltage settings, but their performance characteristics varied significantly. The coordinate-based search method exhibited faster convergence, requiring fewer iterations (e.g., 59 iterations for Problem 1 and 50 iterations for Problem 2) compared to hyperspherical search method. This efficiency is attributed to its systematic exploration of the design space along individual dimensions. However, CD's reliance on local refinement can sometimes limit its ability to escape suboptimal solutions, especially in highly nonlinear

Table 4. Optimization results for problem (2)

N	Method	Optimal solution			Time, s	Iter.
		v*, m/v	(dr*, hs*, hc*, lr*, lc*), m	U*, V		
1	CD	82.1192	(0.0405, 0.0035, 0.00712500, 0.0285, 0.011)	24	1.28	36
	HS	82.2050	(0.04126334, 0.00385087, 0.00702927, 0.02812142, 0.01099913)	12	4.04	40
2	CD	82.1192	(0.0405, 0.0035, 0.007125, 0.0285, 0.011)	12	1.35	36
	HS	81.5673	(0.04089458, 0.00376294, 0.00732296, 0.03166306, 0.01163331)	12	3.46	36
3	CD	82.1192	(0.0405,0.0035, 0.007125, 0.0285, 0.011)	12	1.32	36
	HS	82.1088	(0.04054974, 0.00373675, 0.00737312, 0.02881029, 0.0116334)	12	3.64	39

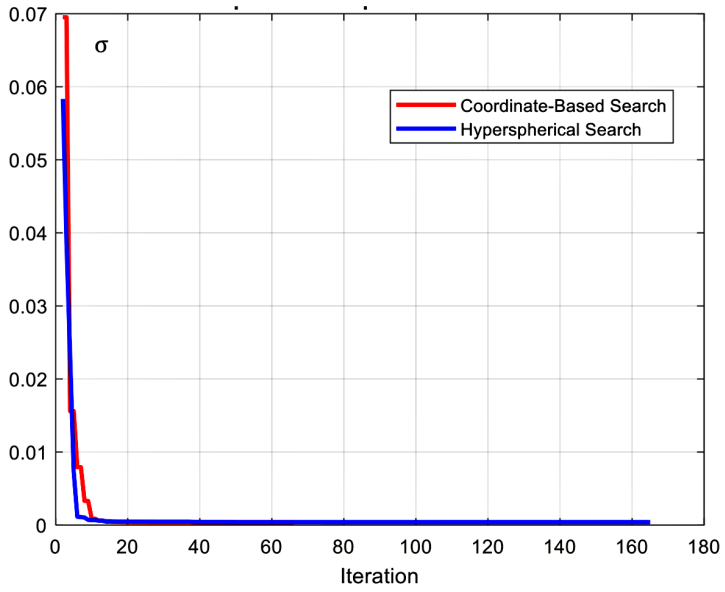

Figure 5. Evolution of the objective function σ

landscapes. In contrast, the HS method required more iterations (e.g., 123 iterations for Problem 1 and 53 iterations for Problem 2) but demonstrated superior global exploration capabilities. This characteristic is advantageous for complex, high-dimensional problems where the objective function may exhibit multiple local minima.

The study also compared two optimization techniques. When using the automated system, the computation time for solving optimization problems was relatively high, ranging from 18.71 to 154.74 seconds per trial. This is due to the iterative nature of the direct and inverse modeling processes, which involves solving nonlinear equations for each candidate solution. While this approach ensures high accuracy, as it relies on physics-based models, its computational demands make it less suitable for real-time applications or large-scale simulations. Machine learning models, such as the TNN for predicting P_E and the Fine Tree method for predicting v, significantly reduced computational time. For example, the TNN model achieved prediction times as low as 0.55 seconds for Problem 1, while the Fine Tree method yielded computation times ranging from 1.28 to 4.04 seconds. These results highlight the potential of machine learning to accelerate optimization processes without compromising accuracy, making it ideal for scenarios where rapid decision-making is critical.

A comparative analysis of the two optimization strategies highlights a trade-off between accuracy and computational efficiency. The automated system, based on detailed physics-driven models, ensures high accuracy, making it suitable for tasks requiring precise validation, such as safety-critical applications or initial design assessments. However, its iterative nature constrains its scalability and increases computational cost. In contrast, machine learning-assisted

optimization significantly reduces computational time, enabling rapid exploration of the design space. Although its accuracy depends on the quality of the training data, the results show that well-trained models can yield near-optimal solutions with minimal error, making this approach highly effective for large-scale or real-time applications.

The integration of heuristic optimization methods with machine learning models presents a promising avenue for advancing MR brake design. By combining the global exploration capabilities of heuristic algorithms with the predictive power of machine learning, researchers can achieve a balance between computational efficiency and solution accuracy. In conclusion, the choice between traditional optimization techniques and machine learning-assisted approaches depends on the specific requirements of the application. While the automated system remains a gold standard for high-precision optimization, machine learning offers a computationally efficient alternative that is well-suited for modern engineering challenges. This efficiency is crucial for real-time applications and large-scale simulations, where computational resources are often limited. Furthermore, the integration of these methods into broader smart engineering systems, including autonomous vehicles and robotics, could unlock new possibilities for MR systems.

CONCLUSIONS

This study demonstrated the application of heuristic and machine learning methods to optimize the performance of magnetorheological brakes. By addressing two key performance indicators: electromagnetic force (P_E) and velocity (v), the research highlights the effectiveness of both traditional optimization techniques and machine learning-assisted hybrid optimization approaches. The analysis showed that, the use of trained neural networks and decision tree models significantly reduced computational time without compromising accuracy, thereby positioning these models as efficient tools for solving complex engineering design and optimization problems. Multi-objective optimization further identified optimal structural parameters and voltage settings, achieving a balance between competing performance metrics. These findings contribute to advancing MR brake technology, emphasizing the importance of integrating advanced modeling and intelligent control strategies. Future work may focus on adapting these approaches to a broader range of electromagnetic systems, with particular emphasis on MR-based devices, and on overcoming real-time implementation barriers to ensure their feasibility in practical engineering applications. The proposed hybrid methods will be incorporated into the automated design and control systems of electromagnetic devices. The optimization framework will be expanded with evolutionary algorithms to further reduce computational time, and for multi-criteria problems additional approaches - such as the weighted-coefficients method - will be implemented. At the same time, the set of machine learning algorithms will be broadened to enhance prediction accuracy. For other investigated devices, new datasets will be constructed to enable the effective application of the proposed hybrid methodology.

Acknowledgement

This work was supported by the Higher Education and Science Committee of Republic of Armenia, in the frames of the research project №25RG-2B089.

REFERENCES

1. Wu J., Kong W., Huang Y., Huang H. Design and experimental evaluation of a multi-drum magnetorheological brake with side-set dual-coil. Alexandria Engineering Journal, 2024; 108: 549–560. https://doi.org/10.1016/j.aej.2024.07.114
2. Abdalaziz M., Sedaghati R., Vatandoost H. Design optimization and experimental evaluation of a large capacity magnetorheological damper with annular and radial fluid gaps. Journal of Intelligent Material Systems and Structures, 2023; 34(14): 1646–1663. https://doi.org/10.1177/1045389X221151075
3. Tharehallimata G., Narasimhamu K. Geometric optimisation of double ended magnetorheological fluid damper. International Journal on Interactive Design and Manufacturing, 2023; 17: 1339–1349. https://doi.org/10.1007/s12008-022-01127-1
4. Olivier M., Sohn J. Design optimization and performance evaluation of hybrid type magnetorheological damper. Journal of Mechanical Science and Technology, 2021; 35: 3549–3558. https://doi.org/10.1007/s12206-021-0726-6
5. Jin Z., Yang F., Rui X., Wang J., Jiang M., Liu Y. Multi-objective optimization design and multi-physics simulation analysis of a novel magnetorheological fluid-elastomer damper. Mechanics Based

Design of Structures and Machines, 2024; 1–27. https://doi.org/10.1080/15397734.2024.2434560

6. Vo V., Le H., Do Q., Nguyen Q. Design and experimental test of a self-sealing component for reciprocal motion of MR fluid-based device. Results in Engineering, 2024; 23: 102835. https://doi.org/10.1016/j.rineng.2024.102835
7. Vo V., Le H., Choi S., Nguyen Q., Van V. Design and empirical evaluation of a magneto-rheological fluid-based seal with rectangular and trapezoidal pole head. Journal of Intelligent Material Systems and Structures, 2024; 35(9): 811–821. https://doi.org/10.1177/1045389X241232720
8. Kim M., Yoo S., Yoon D., Jin C., Won S., Lee J. Numerical analysis of the vehicle damping performance of a magnetorheological damper with an additional flow energy path. Applied Sciences, 2024; 14(22): 10575. https://doi.org/10.3390/app142210575
9. Kariganaur A., Kumar H., Arun M. Study on operational temperature of magneto- rheological fluid and design dimensions of magneto-rheological damper for optimization. Engineering Research Express, 2024; 6. https://doi.org/10.1088/2631-8695/ad3896
10. Zare M., Sedaghati R. Topology optimization of adaptive sandwich plates with magnetorheological core layer for improved vibration attenuation. Journal of Sandwich Structures & Materials, 2024; 26(7): 1312–1340. https://doi.org/10.1177/10996362241278231
11. Hu G., Ying S., Qi H., Yu L., Li G. Design, analysis and optimization of a hybrid fluid flow magnetorheological damper based on multiphysics coupling model. Mechanical Systems and Signal Processing, 2023; 205: 110877. https://doi.org/10.1016/j.ymssp.2023.110877
12. Liu Y., Wang Q., Xing X., Jin J., Chen Z. Development and characterization of a magnetorheological damper with low-velocity sensitivity. Mechanics of Advanced Materials and Structures, 2024; 1–12. https://doi.org/10.1080/15376494.2024.2427931
13. Hu G., Zhang L., Ying S., Yu L., Zhu W. Optimization design and braking performance analysis of cylindrical magnetorheological brake with inner and outer fluid flow channels. Physica Scripta, 2025; 100(4): 045536. https://doi.org/10.1088/1402-4896/adc17c
14. Turabimana P., Sohn J. Optimal design and control performance evaluation of a magnetorheological fluid brake featuring a T-shape grooved disc. Actuators, 2023; 12: 315. https://doi.org/10.3390/act12080315
15. Bhat S., Abinesh A., Naveen S., Kumar H., Arun M. Experimental investigation of rotor wound multi disc magneto-rheological fluid brake. Journal of Intelligent Material Systems and Structures, 36(6), 2025, pp. 398–410. https://doi.org/10.1177/1045389X241312271
16. Cao Z., Yang X., Zhu X., Xia Y. Optimal design and experimental study of comb-type disc magnetorheological brake. Measurement, 2024; 229: 114458. https://doi.org/10.1016/j.measurement.2024.114458
17. He L., Wang Q., Dai L., Shen Y., Hua D., Liu X. Design and optimization of squeeze-shear mode MR brake with multi-fluid flow channels based on multi-objective sooty tern optimization algorithm. Smart Materials and Structures, 2024; 33(11). https://doi.org/10.1088/1361-665X/ad83af
18. Xu W., Hu Y., Zhang Y., Wang J. Design of an integrated magnetorheological fluid brake axial flux permanent magnet machine. IEEE Transactions on Transportation Electrification, 2024; 10(1): 1876–1886. https://doi.org/10.1109/TTE.2023.3287925
19. Hu Y., Xu W. A built-in integrated magnetorheological fluid brake permanent magnet synchronous motor. IEEE Transactions on Magnetics, 2023; 59(11): 8201806. https://doi.org/10.1109/TMAG.2023.3274288
20. Wang D., Yang G., Luo Y., Fang S., Dong T. Optimal design and stability control of an automotive magnetorheological brake considering the temperature effect. Smart Materials and Structures, 2023; 32(2). https://doi.org/10.1088/1361-665X/acb1e2
21. Shamieh H., Sedaghati R. Multi-objective design optimization and control of magnetorheological fluid brakes for automotive applications. Smart Materials and Structures, 2017; 26: 125012. https://doi.org/10.1088/1361-665X/aa9452
22. Ren J., Zhou F., Wang N., Hu G. Multi-objective optimization design and dynamic performance analysis of an enhanced radial magnetorheological valve with both annular and radial flow paths. Actuators, 2022; 11: 120. https://doi.org/10.3390/act11050120
23. Keshav M., Chandramohan S. Geometric optimization of magneto-rheological valve using feedforward neural networks for distribution of magnetic flux density inside the valve. Smart Materials and Structures, 2019; 28: 105018. https://doi.org/10.1088/1361-665X/ab34bd
24. Hu G., Zhou F., Zhu W., et al Geometric optimization and performance analysis of radial MR valve using Taguchi orthogonal experiment method. Journal of Mechanical Science and Technology, 2022; 36: 4593–4614. https://doi.org/10.1007/s12206-022-0822-2
25. Lin Z., Wu M. Dynamic characterization of controlled multi-channel semi-active magnetorheological fluid mount. Mechanical Sciences, 2021; 12: 751–764. https://doi.org/10.5194/ms-12-751-2021
26. Shiao Y., Huynh T. Design and optimization of a new flow-mode magnetorheological mount with compact structure and extended workable force. Journal of Intelligent Material Systems and Structures, 2023; 34(20): 2404–2413. https://doi.org/10.1177/1045389X231185256

27. Vizjak J., Hamler A., Jesenik M. Design and optimization of a spherical magnetorheological actuator. Mathematics, 2023; 11: 4098. https://doi.org/10.3390/math11194098
28. Liu G., Hu H., Ouyang Q., Zhang F. Multi-objective optimization design and performance comparison of magnetorheological torsional vibration absorbers of different configurations. Materials, 2023; 16: 3170. https://doi.org/10.3390/ma16083170
29. Stalin S., Uthayakumar M., Balamurugan P., Pethuraj M., Sładek J., Niemczewska-Wójcik M. Synthesis of silicone oil based magnetorheological fluid and performance analysis in a landing gear using bat-based gradient boost mechanism. Advances in Science and Technology Research Journal, 2025; 19(5): 375–389. https://doi.org/10.12913/22998624/202704
30. Patel D., Upadhyay R., Bhatt D. Design and optimization of shear mode MR damper using GRG and GRA methods: Experimental validation. Sādhanā, 2021; 46: 217. https://doi.org/10.1007/s12046-021-01746-6
31. Kowol P., Sciuto G. Lo, Brociek R., Capizzi G. Magnetic characterization of MR fluid by means of neural networks. Electronics, 2024; 13(9): 1723. https://doi.org/10.3390/electronics13091723
32. Kowol P., Szczygieł M., Sciuto G. Lo, Capizzi G. Modeling of Magnetorheological Fluids Relative Magnetic Permeability by using a Neural Network approach. 2020 IEEE 20th Mediterranean Electrotechnical Conference (MELECON), Palermo, Italy, 2020; 25–28. https://doi.org/10.1109/MELECON48756.2020.9140517
33. Sciuto G. Lo, Kowol P., Pilśniak A. Automated measurements and characterization of magnetic permeability in magnetorheological fluid. Microfluidics and Nanofluidics, 2022; 26(8): 55. https://doi.org/10.1007/s10404-022-02565-9
34. Sciuto G. Lo, Kowol P., Capizzi G. Modeling and experimental characterization of a clutch control strategy using a magnetorheological fluid. Fluids, 2023; 8(5): 145. https://doi.org/10.3390/fluids8050145
35. Sciuto G. Lo, Bijak J., Kowalik Z., Kowol P. Magnetorheological fluid magnetic spring harvester design and characterization. Advances in Science and Technology Research Journal, 2025; 19(5): 128–141. https://doi.org/10.12913/22998624/200857
36. Wei X., Yan T., Liu S. Multi-objective optimization design of magnetorheological damper and vehicle handling stability performance research. Journal of Intelligent Material Systems and Structures, 2023; 35(2): 206–217. https://doi.org/10.1177/1045389X231195835
37. Jiang M., Rui X., Yang F., Zhu W., Zhang Y. Multi-objective optimization design for a magnetorheological damper. Journal of Intelligent Material Systems and Structures, 2021; 33(1): 33–45. https://doi.org/10.1177/1045389X211006907
38. Gurubasavaraju T., Sachidananda K., Narasimhamu K., et al. Perfor-mance evaluation and optimization of magnetorheological damper with non-magnetic spacer using JAYA and grey wolf optimi-zation. International Journal on Interactive Design and Manu-facturing, 2024; 18: 555–567. https://doi.org/10.1007/s12008-023-01579-z
39. Rashidi Meybodi M., Bahar A., Pozo F. Magnetorheological damper parameter identification using a novel metaheuristic algorithm. Mathematical Methods in the Applied Sciences, 2022; 45(17): 10798–10827. https://doi.org/10.1002/mma.8418
40. Yerrawar R., Arakerimath R. Parametric Analysis of Magneto-rheological Strut for Semiactive Suspension System Using Taguchi Method. Engineering, Technology & Applied Science Research, 2018; 8(4): 3218–3222. https://doi.org/10.48084/etasr.2139
41. Dai L., Lu H., Hua D., Liu X., Wang L., Li Q. Research on control strategy of a magnetorheological fluid brake based on an enhanced gray wolf optimization algorithm. Applied Sciences, 2022; 12: 12617. https://doi.org/10.3390/app122412617
42. Shehata Gad A., El-Zomor H. Semi-active suspension design for truck using pneumatic spring joining MR fluid damper based on neural networks controller. SAE International Journal of Vehicle Dynamics, Stability, and NVH, 2025; 9(1): 3–32. https://doi.org/10.4271/10-09-01-0001
43. Grigoryan A., Avetisyan A., Melkonyan T. Parametric study of a hybrid mathematical model of an electromagnetic systems with a magnetorheological fluid. International Review of Electrical Engineering. 2024; 19(2): 60–70. https://doi.org/10.15866/iree.v19i1.24117
44. Grigoryan A., Avetisyan A., Melkonyan T., Hovhannisyan A., Hovsepyan A. Optimization of parameters of electromagnetic system with magnetorheological fluid. International Review of Electrical Engineering, 2024; 19(5): 410–420. https://doi.org/10.15866/iree.v19i5.25645
45. Grigoryan A., Avetisyan A., Chukhajyan N., Hovhannisyan A., Hovsepyan A. Optimal design of an electromagnet using machine learning methods. International Review of Electrical Engineering, 2024; 19(4): 337–345. https://doi.org/10.15866/iree.v19i1.24117
46. Grigoryan A., Avetisyan A., Melkonyan T., Yenokyan K. Automated modeling of an electromagnet with magnetorheological fluid. Engineering, Technology & Applied Science Research. Jun. 2025; 15(3): 22937–22944. https://doi.org/10.48084/etasr.10909